Riset Geologi dan Pertambangan
Earth science journal · Open access · BRIN Earth Sciences & Maritime · BRIN Publishing
ISSN 0125-9849 e-ISSN 2354 6638

RESEARCH ARTICLE
OPEN ACCESS

Riset Geologi dan Pertambangan (2026) Vol. 36, No. 1, 111–124
DOI: 10.55981/risetgeotam.2026.1473

Keywords:
Geochemistry
Mineralogy
Bauxite
Alumina
Red mud

Corresponding author:
Hamzah Lazuardy Zulqisthie
Hamzah21001@mail.unpad.ac.id

Article history:
Received: 15 September 2025
Revised: 13 October 2025
Accepted: 24 October 2025

Author Contributions:
Conceptualization: EE, AP, HLZ
Data curation: EE, HLZ
Formal analysis: HLZ, DW
Funding acquisition: EE, WW, PS
Investigation: HLZ
Methodology: EE, HLZ
Supervision: EE, AP
Visualization: HLZ
Writing – original draft: HLZ
Writing – review & editing: HLZ, EE, AP, WW, DW, PS

Citation:
Zulqisthie, H.L., Ernowo, E., Patonah, A., Widodo, W., Widhiatna, D., Sendjaja, P., 2026. Mineralogical and geochemical characteristics of bauxite ore in stockpile, alumina, and red mud in the Kendawangan area, West Kalimantan, Indonesia. J. Ris. Geol. Pertamb., 36 (1), 111–124, doi: 10.55981/risetgeotam.2026.1473

Mineralogical and geochemical characteristics of bauxite ore in stockpile, alumina, and red mud in the Kendawangan area, West Kalimantan, Indonesia

Hamzah Lazuardy Zulqisthie[1], Ernowo Ernowo[2], Aton Patonah[1], Wahyu Widodo[2], Denni Widhiyatna[3] Purnama Sendjaja[2]

[1] Faculty of Geological Engineering, Padjadjaran University, Indonesia
[2]National Research and Innovation Agency, Indonesia
[3]Center for Mineral, Coal, and Geothermal Resources, Indonesia

Abstract

Mineralogical and geochemical characterization of bauxite ore in stockpile, alumina, and red mud in Kendawangan, Ketapang Regency, West Kalimantan, are conducted to determine the mineral composition, chemical composition, analyze the correlation between mineralogy and geochemistry, and identify the potential of vanadium (V) elements at each stage of the processing of bauxite ore in stockpiles using the X-Ray Diffraction (XRD) and X -Ray Fluorescence (XRF) methods. The results shows that the three types of samples, such as bauxite ore in stockpile, alumina, and red mud. The highest gibbsite mineral and Al_2O_3 content is found in the alumina sample, with >95% gibbsite and 98.74% Al_2O_3, followed by the washed sample from the bauxite ore in stockpile with gibbsite at 92.60% and Al_2O_3 at 56.17%, while the lowest content is found in the red mud sample with gibbsite <1% and Al_2O_3 at 8.11%. Correlation analysis reveals a positive relationship between the main minerals (gibbsite, quartz, kaolinite, and hematite) and the three main oxide compounds (Al_2O_3, SiO_2, and Fe_2O_3). In addition, another correlation analysis exhibits a very strong negative relationship between Al_2O_3 and SiO_2 (R^2=0.78), confirming that the alumina enrichment process occurs through the removal of silica in the washing and Bayer processes. Furthermore, the enrichment of vanadium (V) in the form of V_2O_5 is found in red mud, reaching a maximum concentration at 0.19%.

1. Introduction

Bauxite is the main ore for the global aluminium industry. The benefits are vital, as bauxite is the only source of raw material to produce alumina (Al_2O_3) through the Bayer process, which is then electrolyzed into aluminium metal. Aluminium itself is a strategic commodity that supports various modern industrial sectors, ranging from automotive, construction, aerospace, to packaging (Gow and Lozej, 1993; Suherman et al., 2015). To understand the distribution and quality of its resources, it is important to recognize the process of its formation.

Bauxite is a residual deposit resulting from the intensive chemical weathering process (laterization) of parent rocks rich in aluminosilicate minerals, such as granite and granodiorite (Aprillia et al., 2024; Evans, 1993; Valeton, 1972). Based on the parent rocks type, bauxite can be divided into laterite and karst. Lateritic bauxite accounts for about 85% of the world's bauxite production, this type is formed from the weathering of various types of rocks other than carbonate rocks (Aprillia et al., 2024; Gow and Lozej, 1993). The lateritic process is influenced by several factors including a climate with high rainfall and warm temperatures to accelerate chemical reactions, suitable bedrocks, good drainage, and tectonic stability (Gow and Lozej, 1993; Nurlela et al., 2024). There is a progressive desilication process during in the weathering, where rainwater dissolves and carries away unstable minerals such as silica (SiO_2) from feldspar and mica, while insoluble aluminium will be left behind and concentrated. These insoluble aluminium hydroxide accumulations such as gibbsite ($Al(OH)_3$), boehmite (γ-AlO(OH)), and diaspore (α-AlO(OH)) form bauxite deposits (Gow and Lozej, 1993; Syaputra and Santoso, 2024). This process causes the enrichment of immobile elements such as aluminium and iron due to the washing of other elements, resulting in deposits that are concentrated in certain zones. This chemical weathering process takes place intensively in the tropics and subtropics, resulting in a typical laterite profile consisting of a layer of top soil, followed by a layer of bauxite, a saprolite zone (a rock that has weathered but still shows the texture of the original rock), and at the very bottom is a fresh bedrock (Ramadhan et al., 2014; Syaputra and Santoso, 2024; Valeton, 1972).

In addition to aluminium, bauxite deposits also contain other economic elements such as Gallium (Ga), Titanium (Ti), and Vanadium (V). These elements, although in minor concentrations, can be concentrated in tailing or processing waste (Burke et al., 2012; Damayanti and Khaerunissa, 2017; Praja et al., 2025). Vanadium is one of the critical minerals widely used in high-strength steel alloys, industrial catalysts, and aerospace applications, so its potential in the bauxite industrial process stream is very interesting to explore (Moskalyk and Alfantazi, 2003; Nabilah, 2022; Rizal and Idrus, 2024).

This economic potential of bauxite is very relevant for Indonesia, which holds a strategic position on the world bauxite potential, with 7.48 billion tons resources and 2.78 billion tons reserves (Kementerian ESDM, 2024). The bauxite in West Kalimantan Province, where the research area is located in Ketapang Regency (Figure 1), accounts for more than 66% of the national reserves and making it a vital center for the alumina industry in Indonesia (Kementerian ESDM, 2024). The characterization of geological resources using integrated mineralogical and geochemical approaches by combining XRD for phase identification and XRF for bulk chemistry has been established as an effective methodology for evaluating mineral deposits and industrial minerals in Indonesia (Setiawan et al., 2020; Lintjewas et al., 2019).

However, these are two main challenges in managing these resources. First, the variability of ore quality from bauxite as a raw material, such as Al_2O_3, Fe_2O_3, and other impurities, will directly have an impact on the decline in the quality of raw materials and Bayer process results (Dubovikov and Jaskelainen, 2016; Purnomo and Wijaya, 2022; Syaputra and Santoso, 2024). Second, the red mud, which is tailing from the Bayer process, has a high potential to pollute the environment due to its heavy metal content, highly alkaline nature, and massive volume of 0.8 to 1.5 tons for every ton of alumina produced (Jaya et al., 2020; Santi, 2019; Zaharah T. A et al., 2021). The existence of these two main challenges requires a comprehensive study of the relationship between the mineralogical and geochemical quality of the stockpile and the quality of the products (alumina and red mud).

While many studies have focused on either raw bauxite characterization or red mud management, this research provides a novel, integrated perspective by meticulously tracking the mineralogical and geochemical transformations across the entire processing chain from stockpile ore to purified alumina and residual red mud. This study aims to not only characterize these materials but also to analyze their inter-correlations, with a specific evaluation of the distribution pathway of vanadium (V_2O_5). Therefore, the primary contribution of this research is to bridge the gap between upstream resource quality and downstream process outcomes, providing a scientific basis for optimizing raw material blending and creating a circular economy model through the valorization of critical minerals from industrial waste.

2. Regional Geology

The study area is part of Schwaner Block (Van Bemmelen, 1949), which physiographically is composed of a complex of igneous and metamorphic rocks. This block is dominated by Cretaceous granitoid rocks that intrude metamorphic rocks from the Pinoh Metamorphic Group (Auliya et al., 2021; Breitfeld et al., 2020; Setiawan et al., 2013; Williams et al., 1988). The Schwaner Mountains are the Pre-Tertiary basement which is the source of sedimentary material in the Barito Basin located to the east (Heryanto and Margono, 2008). The existence of felsic igneous rocks rich in aluminosilicate minerals from the Schwaner Block is the main key as the parent rock of lateritic bauxite deposits in the study area (Auliya et al., 2021; Heryanto and Margono, 2008).

The formation of the Schwaner Block is closely related to the subduction activity of the Paleo-Pacific plate under Southwest Borneo during the Mesozoic Era (Breitfeld et al., 2020). This tectonic process produces a magmatic arc that stretches from Schwaner to Singkawang, producing metaluminous type-I igneous rocks with high calc-alkaline to potassium calc-alkaline affinity (Auliya et al., 2021; Batara and Xu, 2022). The igneous rocks resulting from this subduction activity mainly formed in the Cretaceous Period, ranging from 144 to 72 million years ago (Batara and Xu, 2022). The intensive weathering process in granite and tonalite rocks then forms alumina-rich residues as the precursors of the bauxite deposits (Heryanto and Margono, 2008).

The significance of the Schwaner Block as a source rock is confirmed by the composition of the surrounding sedimentary rocks, such as the Eocene Cape Formation. The sandstone petrology of the formation shows rock fragments originating from the Continental Block (Interior Craton), which refers to the Pre-Tertiary rocks of the Schwaner Mountains. The composition of granite, limestone, and metamorphic rocks rich in the feldspar and mica are the main sources of aluminosilicate materials (Heryanto and Margono, 2008).

The physiography of the Schwaner Block is also in correlates with the regional geological conditions on the Regional Geological Map of the Kendawangan Sheet (Sudana et al., 1994; Figure 1). The research area location in the Sukadana Granite Formation (Kus) with Early Cretaceous to the Late Cretaceous. This formation is dominantly composed of granite, diorite, and granodiorite with a fresh reddish-gray to blackish-gray color. Moreover to the Sukadana Granite formation, there are other formations that surround it, such us the Kerabai Volcanic Rock Formation (Kuk) and the Swamp Sediment Formation (Qs) (Sudana et al., 1994). The existence of the Sukadana Granite Formation as the dominant bedrock unit at the research site strengthens the direct relationship between magmatic activity in the Schwaner Block and the presence of exploited bauxite deposits. Therefore, bauxite is the main commodity of interest in the research area.

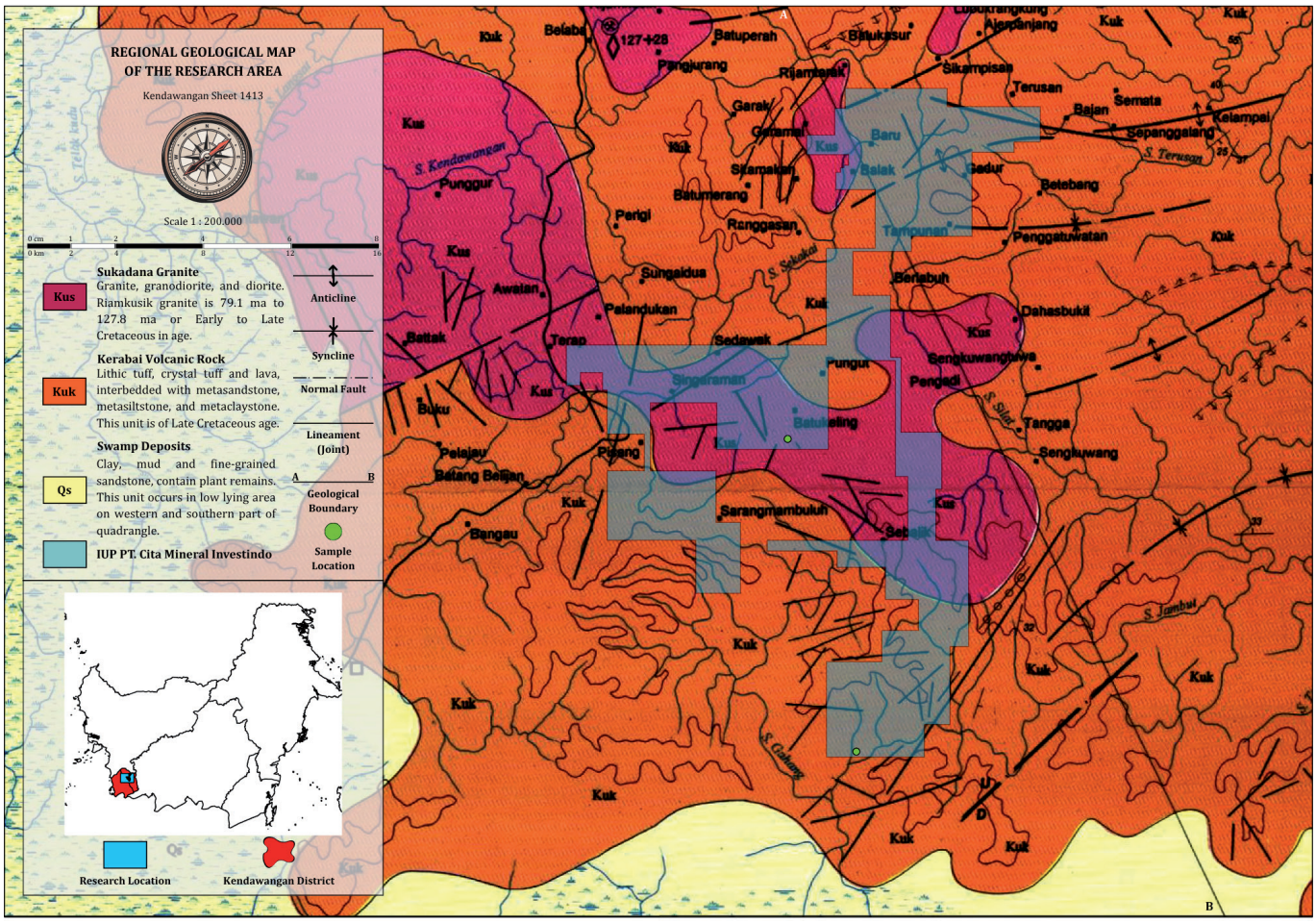

Figure 1. Regional geological map with the research location of the IUP of PT. Cita Mineral Investindo (Modified from Sudana et al., 1994).

3. Data and Methods

Samples were collected from the stockpile of PT. Cita Mineral Investindo (CMI) on Friday, January 24, 2025. The sampling strategy followed the processing flow from PT. CMI (Figure 2). Nine samples were representing the bauxite processing workflow, consisting of ore (O), concretion (K), clay (C), washed (W), settling pond (P), accepted residue (R), disposal or rejected residue (D), alumina (A), and red mud (RM).

The ore sample (raw bauxite) is an initial unprocessed material. In this study, the ore sample was screened by grain size, a process that results in two fractions; a concretion sample that retained on a #20 mesh (≥841 mm) and a clay sample that passes through it (<841 mm). These two fractions are then washed separately in different places. The concretion sample is washed in the washing plant producing a washed sample, while the clay sample is washed in the settling pond producing a settling pond sample. After that, the settling pond sample is then separated into accepted residue and disposal (rejected residue) samples. Finally, the washed sample and the accepted residue sample that had passed the company specifications were processed using the Bayer process to produce an alumina sample as a main product and a red mud sample as a tailing product.

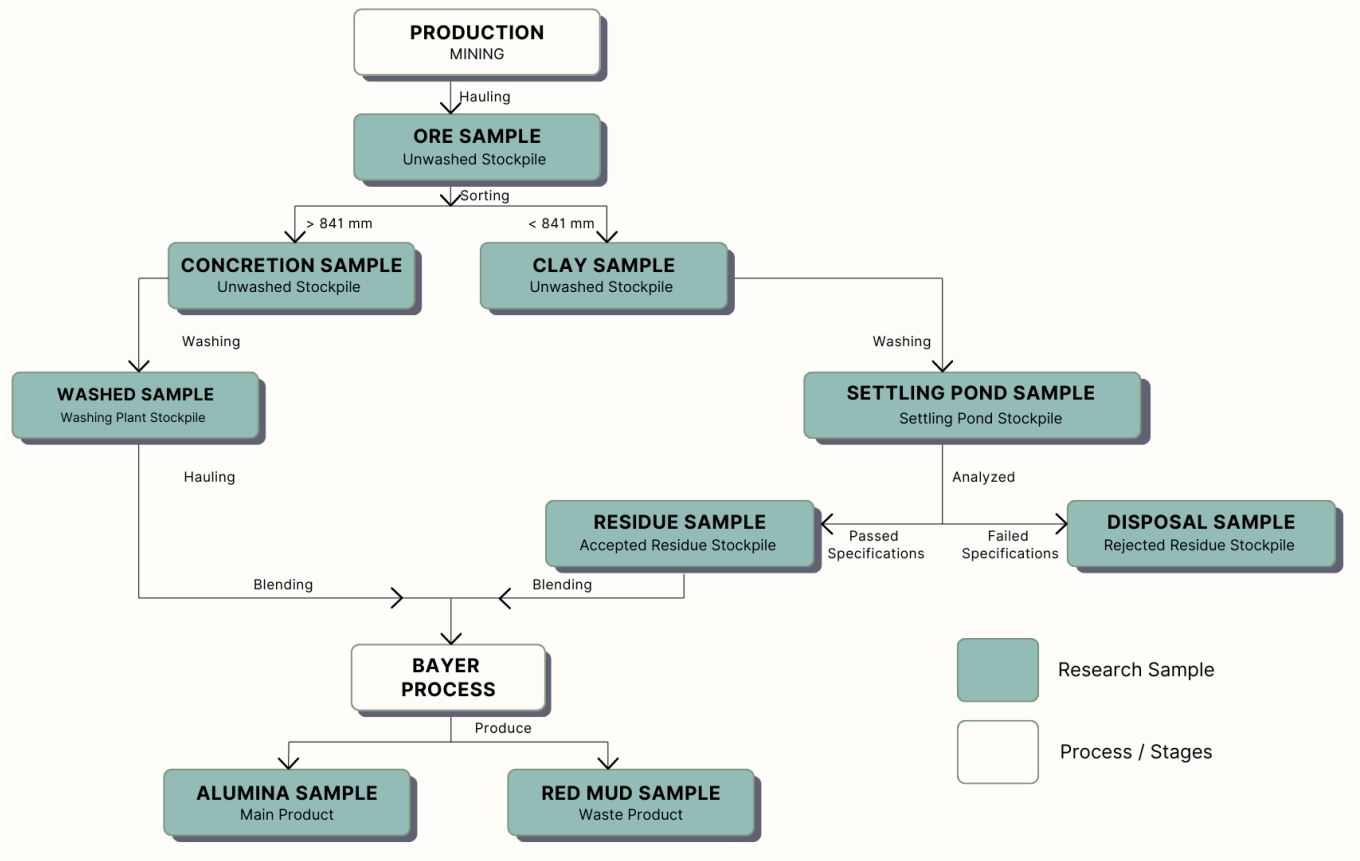

Figure 2. Flowchart illustrating of the research sampling points along the bauxite processing (Modified from PT. Cita Mineral Investindo).

Each sample was prepared by drying and grinding until it reaches a fine powder size (<200 mesh) to ensure homogeneity. Subsequently, the prepared samples underwent mineralogical and geochemical analyses. The mineralogical analysis was conducted to determining the mineral composition (gibbsite, quartz, kaolinite, hematite, sodalite, and rutile) using an X-Ray Diffraction (XRD) Bruker D8 Advance Eco instrument at the BRIN Ionizing Radiation Laboratory. This integrated approach of combining XRD and XRF analysis has been widely applied in characterizing geological materials in Indonesia, including studies on laterite deposits (Lintjewas et al., 2019) and zeolite-bearing rocks (Setiawan et al., 2020), demonstrating its effectiveness for resolving mineral composition and geochemical relationships simultaneously. The resulting XRD data were processed using HighScore Plus and Origin software to generate X-ray diffractograms for each sample. Besides that, geochemical analysis was performed to determining the quantitative chemical composition of oxide compounds (Al_2O_3, SiO_2, Fe_2O_3, V_2O_5, MgO, CaO, Na_2O, K_2O, TiO_2, P_2O_5, dan MnO) as well as Loss of Ignition (LOI) and Moisture Content. It was carried out using the X-Ray Fluorescence (XRF) Panalytical Minipal 4 instrument at the laboratory of Center for Mineral, Coal, and Geothermal Resources (PSDMBP). Similarly, XRF has been effectively employed in other mineralogical and geochemical characterization studies in Indonesia, including characterization of red limestone (Atmoko et al., 2016) and engineered geopolymer composites derived from silica-alumina-rich materials (Amin et al., 2023). The results of the XRF analysis were then processed and visualized using charts from Microsoft Office software to illustrate compositional variations among the samples.

4. Results

The XRD results reveal the content of various minerals in percentage (%). The primary minerals detected include gibbsite, quartz, kaolinite, hematite, sodalite, and rutile (Figure 3). The gibbsite content in the ore sample (O) is 67.7%. After the screening process, this content increases to 86.6% in the concretion sample (K) but decreases to 35.3% in the

clay sample (C). The washing step proves highly effective, significantly raising the gibbsite concentration in the washed sample (W) to 95.4%, thus meeting the specifications for the Bayer process. Furthermore, the gibbsite content in the settling pond sample (P) is 76.9% and also considerably higher than that of the initial clay. After separation, the accepted residue (R) contains 81% gibbsite, while the content in the disposal sample (D) drops to 26.9%. Following the Bayer process, gibbsite is no longer detected in the red mud (RM), as it is fully consumed to produce alumina.

Conversely, the quartz and kaolinite content showing an inverse trend relative to gibbsite. The O-sample starts with 3.9% quartz and 28.4% kaolinite. After screening process, the concentration of these minerals decreases in the K-sample (8.6% quartz and 2.7% kaolinite), but increases in the C-sample (15.2% quartz and 49.5% kaolinite). The washing process in W-sample effectively reduces up to 0.7% quartz and 2.9% kaolinite. Correspondingly, the P-sample contain 15.8% quartz and 5.7% kaolinite. At the R-sample quartz and kaoline are 8.7% and 8.8%, respectively. Kaolinite was highly concentrated in the D-sample to reach 34.6% with additional 37.6% quartz. Finally, the RM-sample contains 5.1% quartz and negligible amount of kaolinite.

Regarding hematite, its content in the O-sample is very low (<1%). After screening, there is a slight increase to 2.1% in the K-sample and decrease to <1% in the C-sample. Unlike quartz and kaolinite, the washing process does not significantly reduce hematite, with 1% concentration in the W-sample remains. The hematite content shows an increasing trend in the P-sample (1.6%) while decreasing in the R-sample (1%). The peak concentration occurs after the Bayer process, where the hematite becomes a dominant component in RM-sample at a very high concentration of 67.4%. Additionally, other minerals, such us sodalite (24.8%) and rutile (2.3%), are identified exclusively in the RM-sample.

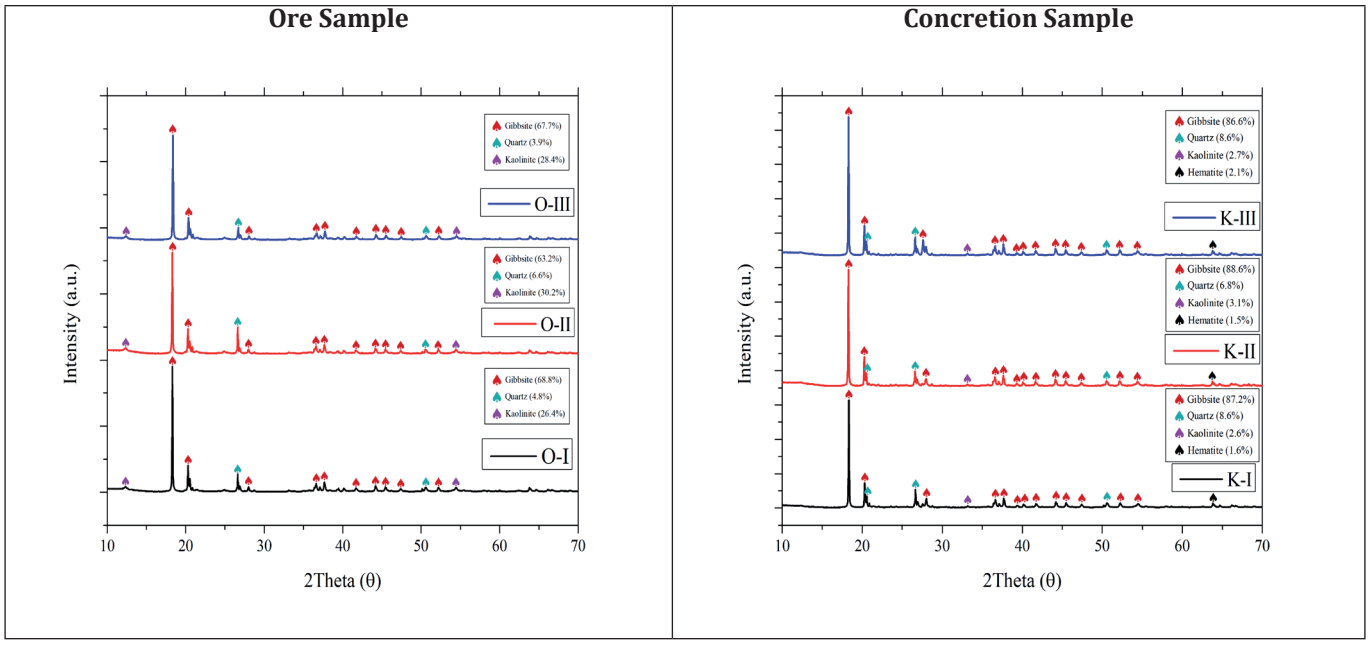

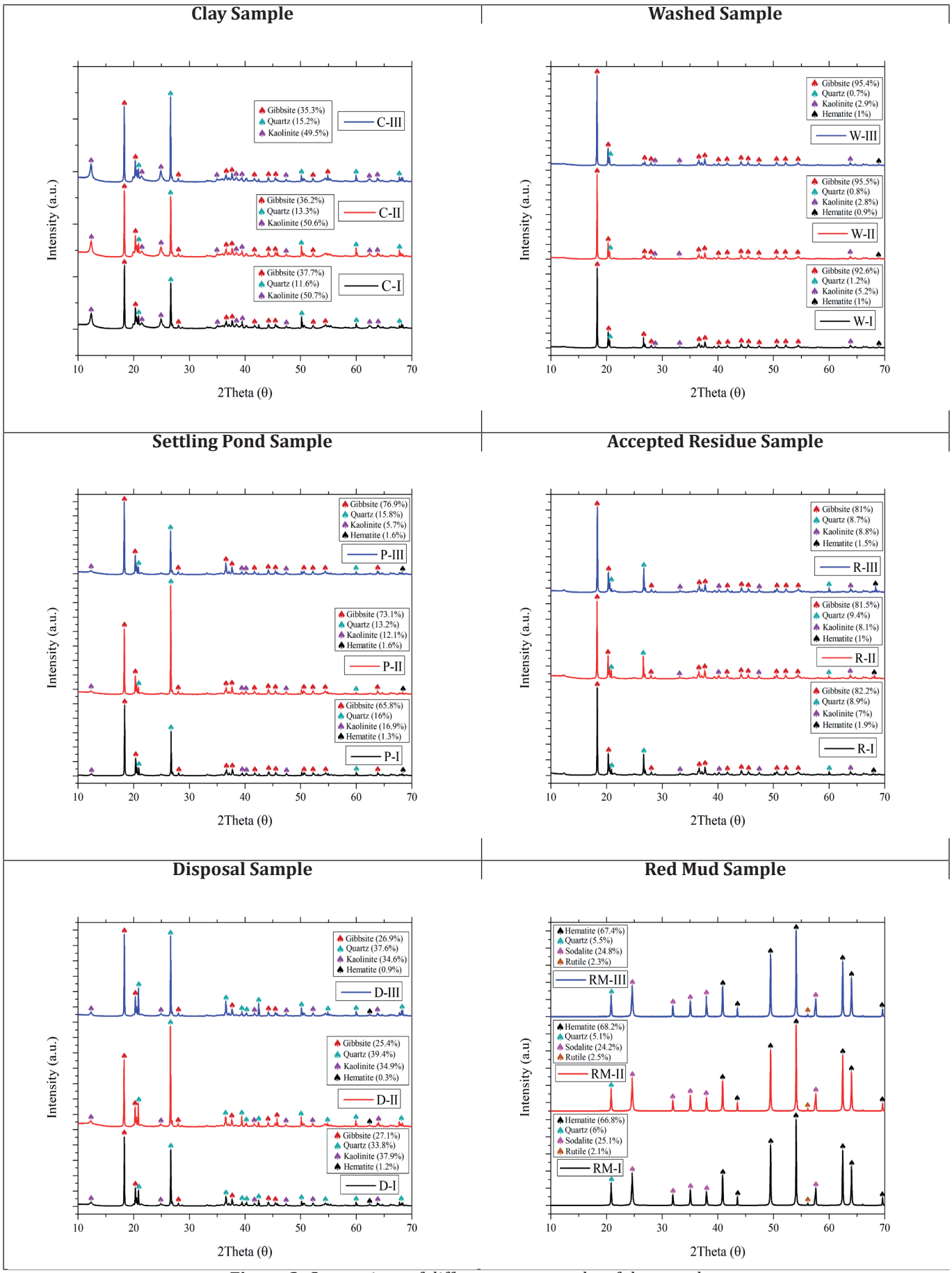

Figure 3. Comparison of diffractometry graphs of the samples.

XRD analysis of the various samples reveals the mineral distribution at each stage of the processing workflow, from the initial ore in stockpile to the final alumina and red mud products (Figure 4).

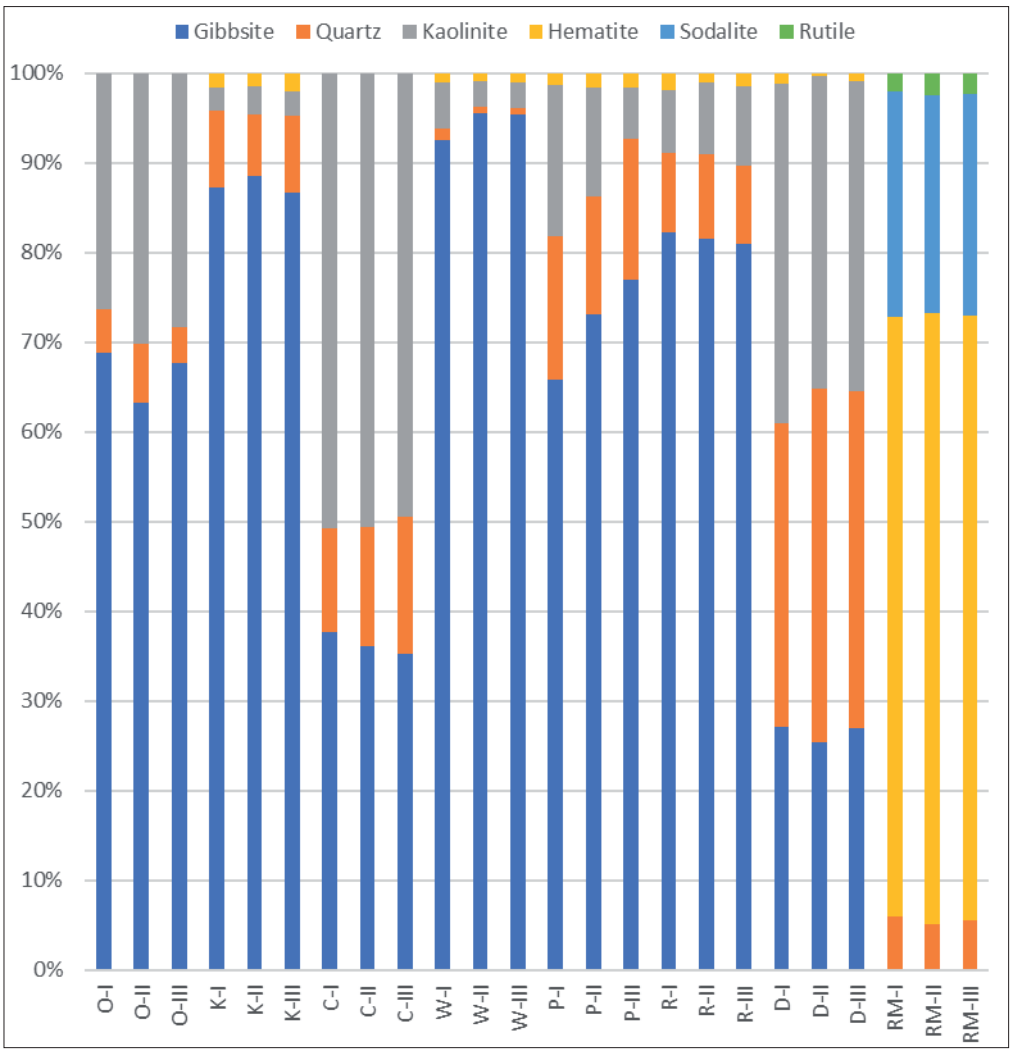

Figure 4. Quantitative Mineralogy Based on XRD Analytical Results (O=Ore, K=Concretion, C=Clay, W=Washed, P=Settling Pond, R=Accepted Residue, D=Disposal, A=Alumina, RM=Red Mud).

The results of the mineral composition analysis from XRD are confirmed and deepened through XRF analysis to determine the specific chemical compounds present. The quantitative XRF analysis reveals significant variations in the oxide compound content at each processing stage (Table 1). The following sections detail the distribution trends of the major oxides (Al_2O_3, SiO_2, Fe_2O_3) and the notable enrichment of a key minor element, V_2O_5. (Figure 5). The Al_2O_3 content in the O-sample is 42.33%. After screening process, this content in the K-sample increases to 42.80%, but decreases in the C-sample to 39.10%. The washing step proves highly effective, significantly raising the gibbsite concentration in the W-sample to 95.4%, thus meeting the specifications for the Bayer process. Furthermore, the Al_2O_3 content in the P-sample (76.9%) is also considerably higher than that of the initial clay. After separation, the R-sample contains 81% Al_2O_3, while the content in the D-sample drops to 26.9%. Following the Bayer process, the Al_2O_3 concentration peaks at 98.74% in the A-sample, and decrease significantly to 8.11% in RM-sample.

Conversely, the SiO_2 content show an inverse trend relative to the Al_2O_3. The O-sample starts with 27.65%. After screening process, the K-sample slightly decreases to 26.31% in the concretion sample but increases to 32.17% in the C-sample. The washing process effectively reduces the content in W-sample up to 3.23%. Correspondingly, samples from the P-sample contains 22.21% SiO_2. At the separation stage concentration of SiO_2 was decrease to 15.15% but increased to 46.94% in D-sample. Finally, the A-sample contain very low SiO_2, which is 0.01%, while in RM-sample there is still 9.49%.

Regarding Fe2O3, its content in the O-sample is 5.38%. After screening, there is a slight decrease to 4.87% in the K-sample and increase to 6.96% in the C-sample. Unlike silica,

the washing process does not significantly reduce Fe_2O_3, with the level in the W-sample remaining at 6.84%. The Fe_2O_3 content shows an increasing trend in the P-sample (10.04%) and the R-sample (11.15%). The peak concentration occurs after the Bayer process, where Fe_2O_3 becomes a dominant component in RM-sample with a very high concentration of 60.25%. On the other hand, the A-sample is successfully purified until it had a negligible Fe_2O_3 content with only 0.01%.

The geochemical analysis also highlights the distribution of minor elements, particularly V_2O_5. While the V_2O_5 content is very low in the raw and intermediate materials (0.01% - 0.09%), a significant enrichment is observed in the final red mud, where it reaches its highest concentration of 0.19%.

Table 1. X-Ray fluorescence analysis results.

NO	SAMPLE		PARAMETERS												
			V_2O_5	Al_2O_3	SiO_2	Fe_2O_3	MgO	CaO	Na_2O	K_2O	TiO_2	P_2O_5	MnO	LOI	Moisture Content
	CODE	TYPE	%	%	%	%	%	%	%	%	%	%	%	%	%
1	O-I	Ore	0.09	42.33	27.65	5.38	0.39	0.19	0.34	0.38	0.65	0.10	0.04	24.89	0.66
2	K-I	Concretion	0.12	42.80	26.31	4.87	0.43	0.26	0.60	0.54	0.54	0.10	0.04	26.49	0.48
3	C-I	Clay	0.01	39.10	32.17	6.96	0.05	0.01	0.01	0.02	1.12	0.10	0.02	19.43	1.71
4	W-I	Washing Plant	0.01	56.17	3.23	6.84	0.01	0.01	0.14	0.04	0.88	0.09	0.02	30.97	0.60
5	P-I	Settling Pond	0.01	40.49	22.21	10.04	0.01	0.01	0.03	0.08	1.62	0.16	0.04	23.48	0.56
6	R-I	Residue	0.02	43.14	15.15	11.15	0.01	0.04	0.17	0.14	1.91	0.19	0.04	25.96	1.20
7	D-I	Disposal	0.01	17.38	46.94	11.29	0.05	0.01	0.01	0.02	0.86	0.09	0.02	22.36	0.76
8	RM-I	Red Mud	0.19	8.11	9.49	60.25	0.05	1.06	8.46	0.29	3.07	0.58	0.13	22.76	1.10
9	A-I	Alumina	0.0009	98.74	0.01	0.01	0.01	0.01	0.33	0.009	0.01	0.0009	0.001	0.86	1.12

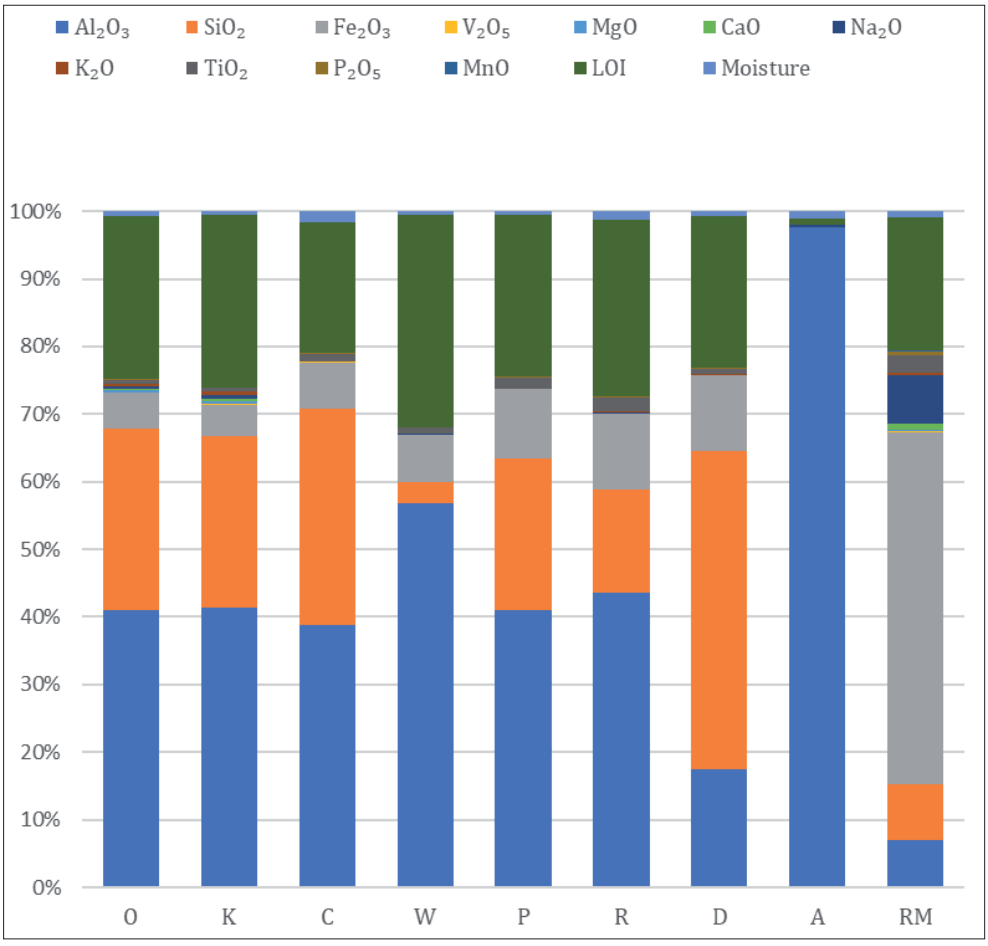

Figure 5. Quantitative geochemistry based on XRF analytical results (O=Ore, K=Concretion, C=Clay, W=Washed, P=Settling Pond, R=Accepted Residue, D=Disposal, A=Alumina, RM=Red Mud).

To understand the relationship between mineralogy and geochemistry of the research samples, the correlation between mineral content and major oxide compounds are presented (Figure 6). The results of the analysis show a strong positive correlation between gibbsite and Al_2O_3 (R^2=0.71), indicating that gibbsite is the primary Al-bearing mineral of aluminium carriers. Furthermore, SiO_2 indicates two distinct positive correlations such a strong correlation with quartz (R^2=0.70) and a weak correlation with kaolinite (R^2=0.38). This implies that the silica is distributed between these two mineral phases. This pattern of oxide-mineral correlation, where major oxides such as SiO_2, Fe_2O_3, and Al_2O_3 show geochemical enrichment trends that reflect their associated mineral carriers, is consistent with findings from other Indonesian geological materials (Atmoko et al., 2016). In contrast, the very weak positive correlation between Fe_2O_3 and hematite (R^2=0.08) suggests the presence of other iron-bearing minerals, such as goethite, not detected in this study. This observation aligns with previous laterite studies using XRD and XRF that identified multiple iron-bearing mineral phases in tropical weathering profiles (Lintjewas et al., 2019).

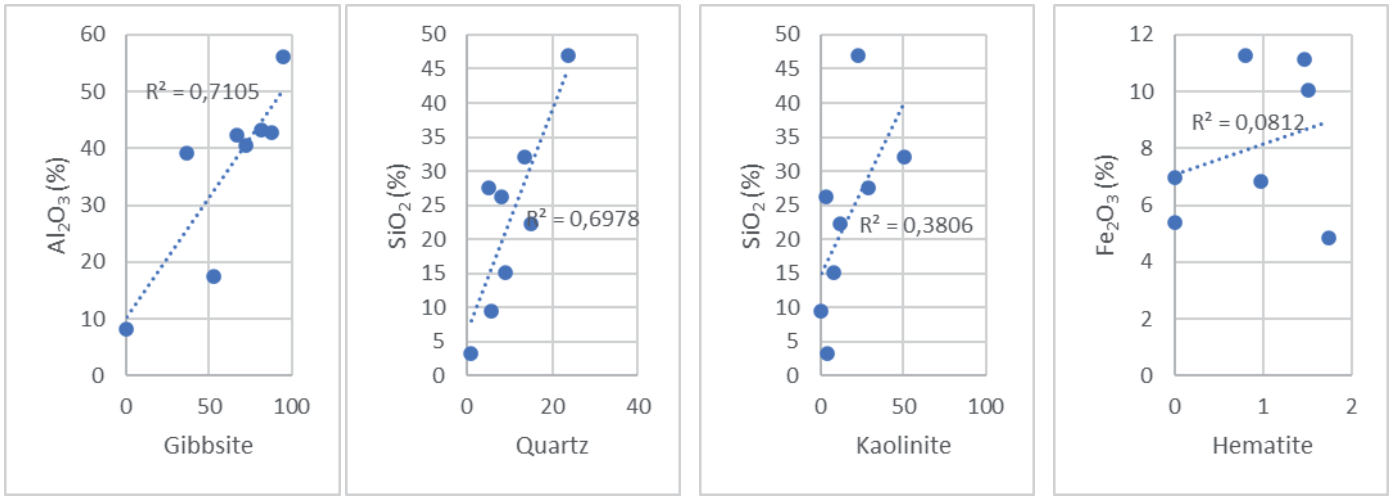

Figure 6. Correlation graph of oxide compounds with minerals.

Furthermore, Correlations between the dominant oxide compounds are examined to understand the geochemical relationships that control element distribution during processing (Figure 7). The results show a strong negative correlation between Al_2O_3 and SiO_2 with a determination coefficient (R^2) of 0.78. Meanwhile, the correlation between Al_2O_3 and Fe_2O_3 is weakly negative correlation with a determination coefficient (R^2) of 0.26, and the correlation between SiO_2 with Fe_2O_3 is negligible with a determination coefficient (R^2) of 0.01.

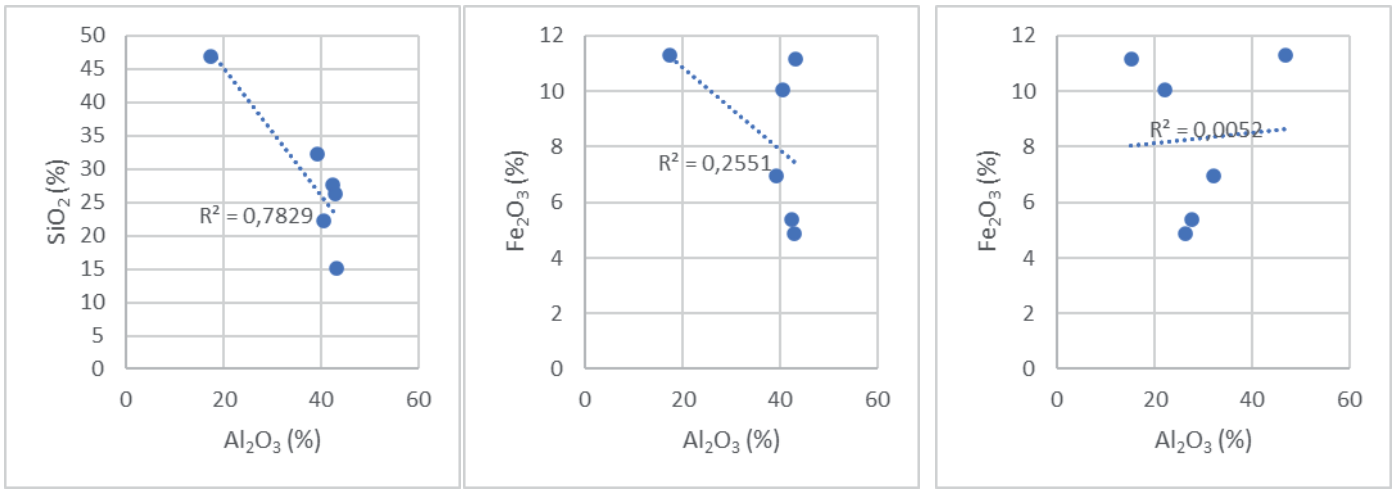

Figure 7. Correlation graph of oxide compounds.

The correlation of vanadium with the dominant compound is also carried out to understand the geochemical behavior and distribution pathways of vanadium during the bauxite processing (Figure 8). The correlation results between V_2O_5 and Al_2O_3 is weakly negative correlation with a coefficient of determination (R^2) of 0.21. In contrast, the correlation

between V_2O_5 and Fe_2O_3 exhibit a very strong positive correlation with a coefficient of determination (R^2) of 0.94. Meanwhile, the correlation results between V_2O_5 and SiO_2 reveal a very low correlation with a coefficient of determination (R^2) of 0.05.

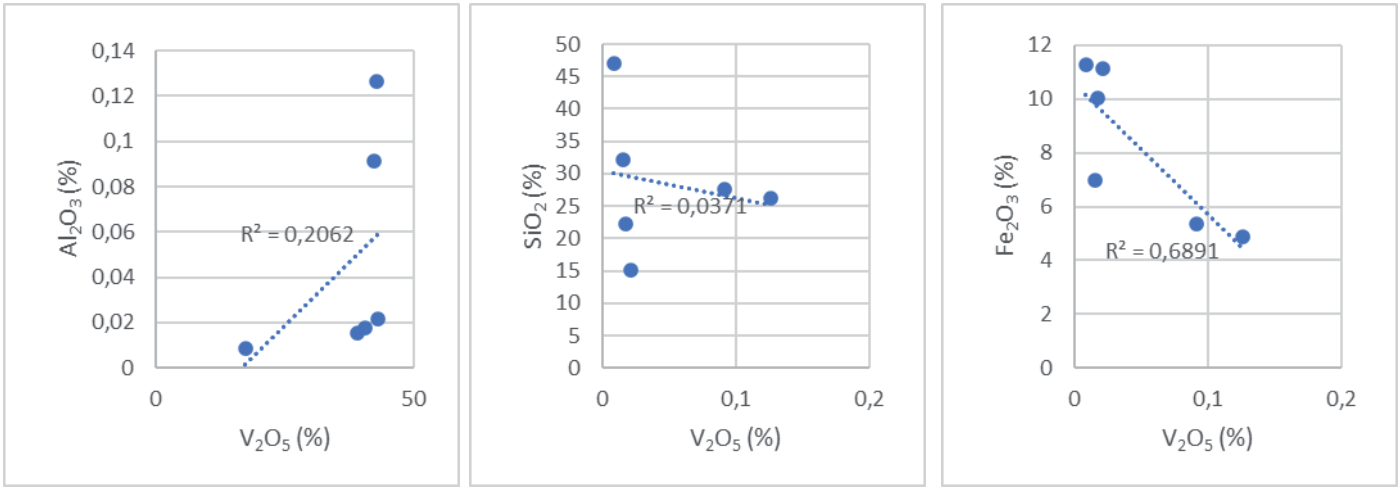

Figure 8. Correlation graph of vanadium with oxide compounds.

5. Discussion

5.1 Increased alumina concentration through silica elimination

The high Al_2O_3 content achieved in the alumina sample (98.74%) and the washed sample (56.17%) demonstrates the effectiveness of the processing workflow. The enrichment is achieved through physical separation during washing and chemical purification through the Bayer process. The washing stage aims to remove non-reactive gangue minerals such as quartz (Gow and Lozej, 1993). Similarly, the Bayer process is the core of modern alumina production. It selectively dissolves the mineral aluminium hydroxide and separates it from insoluble impurities (Fe_2O_3 dan V_2O_5).

The strong negative correlation between Al_2O_3 and SiO_2 (R^2=0.78) highlights the fundamental difference in the geochemical behavior of these elements. Geochemically, aluminum (Al) is immobile element, meaning it tends to be retained and accumulate in residual deposits. In contrast, silica (Si) is mobile element and easily leached by water. This principle of differential mobility is precisely what drives the formation of lateritic bauxite deposits, including those in West Kalimantan (Permatasari et al., 2024). Therefore, the strong negative correlation is not just a statistical artifact but a quantitative confirmation that the efficiency of alumina enrichment is directly proportional to the effectiveness of silica elimination.

5.2 Geochemical affinity of iron and vanadium as determinants of red mud composition

The inert nature of iron minerals during the Bayer process is the main reason for the high concentration of Fe_2O_3 (60.26%) in red mud. In the highly alkaline and high-temperature environment of the Bayer process, iron-bearing minerals such as hematite and goethite are essentially insoluble. As a result, as alumina is selectively dissolved, these iron minerals are left behind as solid residues and become passively concentrated. This characteristic that has also been identified in red mud from other locations in West Kalimantan (Zaharah et al., 2021).

The concentration of V_2O_5 in red mud can be explained by the strong geochemical affinity between vanadium and iron. The very strong positive correlation (R^2=0.94) between these two oxides is not a coincidental, it provides compelling evidence for isomorphic substitution. Due to the size similarities and ionic charge, V^{3+} ions can replace the position of Fe^{3+} ions in the crystal structure of iron oxide minerals (Burke et al., 2012). Vanadium is “locked” in the iron mineral, which is then taken away when the iron mineral builds up in the red mud.

The enrichment of critical minerals such as vanadium in industrial waste streams represents a significant opportunity for circular economy applications. The growing global demand for

critical raw materials, including vanadium used in high-strength alloys and energy storage systems, has intensified interest in recovery from secondary sources such as industrial residues (Solihin et al., 2024). From this perspective, the red mud from the Kendawangan bauxite processing plant, with V_2O_5 concentrations reaching 0.19%, warrants further valorization studies as a potential secondary source of this strategic mineral. Vanadium extraction from red mud can provide significant economic added value, in line with the circular economy principle to maximize the utilization of all ore components (Moskalyk and Alfantazi, 2003).

5.3 Mineralogical and geochemical correlation and inter-oxidation relationships

The positive correlation between the mineralogical (XRD) and geochemical (XRF) data confirms the identity of the primary host mineral for each major oxide. The strong correlations between gibbsite and Al_2O_3, as well as quartz and SiO_2, confirm the dominant role of these minerals, which align with the general characterization of bauxite deposits in Kalimantan (Ramadhan et al., 2014). However, the weaker correlation between hematite and Fe_2O_3, suggest the presence possibility of other iron-bearing minerals, such as goethite.

Correlation between the oxide compounds confirms the geochemical relationships that control the element enrichment and separation during processing. A very strong negative correlation between Al_2O_3 and SiO_2 (R^2=0.78) proves that alumina enrichment occurs in tandem with the process of silica removal (leaching), which is the basic principle of bauxite formation and purification. The weak negative correlation between Al_2O_3 and Fe_2O_3 (R^2=0.26) suggests that although the two tend to separate during the Bayer process (Al solutes, Fe does not), iron tends to accumulate independently and is not directly related to alumina levels. Meanwhile, a very weak correlation between SiO_2 and Fe_2O_3 (R^2=0,01) suggests that the distribution is controlled by independent processes, the concentration of SiO_2 is strongly influenced by the efficiency of physical washing, while the concentration of Fe_2O_3 is more residual and accumulates passively when other components are removed.

5.4 Implications of raw material quality on process efficiency

This analysis establishes a clear causal relationship between the quality of raw materials (stockpile), main product (alumina), and tailing (red mud). The quality of raw materials (inputs) is a critical determinant factor that directly controls the efficiency of the process and the quality of the final product (output). The variability of bauxite quality, as reported in West Kalimantan, is a major operational challenge (Syaputra and Santoso, 2024). The use of high-quality stockpiles, which rich in Al_2O_3 and low in reactive silica, will result in a positive impact of more efficient processes, purer products, and lower tailing volumes. Meanwhile, the use of low-quality bauxite will have negative impacts caused by side reactions from reactive silica. During the Bayer process, kaolinite will dissolve and react with the soda flame solution to form an unwanted desilication product, such as sodalite. This reaction is very detrimental because it consumes expensive sodium hydroxide reagents and causes the loss of a certain amount of alumina trapped in the deposit, thus directly reducing the yield of the product (Dubovikov and Jaskelainen, 2016).

6. Conclusion

The bauxite processing in Kendawangan, West Kalimantan, effectively increases the Al_2O_3 content from 42.33% in the raw ore stockpile to 98.74% in the final alumina product. This enrichment is achieved through the removal of gangue minerals, especially SiO_2. The effectiveness of this removal is demonstrated by the drastic reduction in silica content from 27.65% to only 3.23% after the washing process. Correlation analysis shows a strong inverse relationship between Al_2O_3 and SiO_2 (R^2=0.78), confirming that the efficiency of the alumina enrichment process is highly dependent on the successful elimination of silica.

Red mud, as the main residue of this process, shows a very high concentration of impurities, especially Fe_2O_3 (60.26%). A very strong positive correlation exists between V_2O_5 and Fe_2O_3 (R^2=0.94), confirms that vanadium has a strong geochemical affinity with iron and also concentrated in red mud. With V_2O_5 concentrations reaching 0.19%, this study underscores the potential for further valorization studies to extract vanadium as an economically valuable by-product.

Overall, the quality of raw materials (stockpile) has proven to be a major determining factor for process efficiency and product quality. The higher the quality of the stockpile (high Al_2O_3, low SiO_2), the higher the purity of the alumina produced and the lower volume of red mud produced.

Acknowledgments

The author would like to thank the Research Center for Geological Resources, National Research and Innovation Agency (BRIN) for funding and accommodating the laboratory analysis of X-Ray Fluorescence (XRF) and X-Ray Diffraction (XRD). This research activity was financed from the activities of the Disaster and Earth Resources Research and Innovation Prototype Program, the Mitigation of Sustainable Critical and Strategic Mineral Resources Scarcity Mitigation sub-program at National Research and Innovation Agency (BRIN) and collaboration with Ministry of Energy and Mineral Resources (MEMR).

References

Amin, M., Sudibyo, S., Birawidha, D., Rinovian, A., Erlangga, B., Al Muttaqqi, M., Suka, E., Pratiwi, S., 2023. Effect of bentonite on fly ash and bottom ash based engineered geopolymer composite. Ris. Geol. Pertamb. 33. https://doi.org/10.55981/risetgeotam.2023.1225

Aprillia, R., Mukhtar, W., Setiawati, S., Asbanu, G.C., Munzir, I., 2024. Genesis of bauxite ore in Toba area Sanggau district, West Kalimantan Province. J. Geocelebes 8, 26–36.

Atmoko, D., Titisari, A., Idrus, A., 2016. Mineralogi dan geokimia batugamping merah Ponjong, Gunungkidul, Daerah Istimewa Yogyakarta – Indonesia. Ris. Geol. Pertamb. 26, 55–67. https://doi.org/10.14203/risetgeotam2016.v26.269

Auliya, I., Ramadhan, A., Kivlan, M., Darmaputra, M., Najah, M.B., 2021. Geochemical characteristics of Schwaner Mountains granitoids and their relationship to magmatism in the Southwest Borneo Block. Proc. Joint Conv. Bandung (JCB) 01, 1–6.

Batara, B., Xu, C., 2022. Evolved magmatic arcs of South Borneo: insights into Cretaceous slab subduction. Gondwana Res. 111, 142–164.

Breitfeld, H.T., Davies, L., Hall, R., Armstrong, R., Forster, M., Lister, G., Thirlwall, M., Grassineau, N., Hennig-Breitfeld, J., van Hattum, M.W.A., 2020. Mesozoic Paleo-Pacific subduction beneath SW Borneo: U-Pb geochronology of the Schwaner Granitoids and the Pinoh Metamorphic Group. Front. Earth Sci. 8. https://doi.org/10.3389/feart.2020.00568

Burke, I.T., Mayes, W.M., Peacock, C.L., Brown, A.P., Jarvis, A.P., Gruiz, K., 2012. Speciation of arsenic, chromium, and vanadium in red mud samples from the Ajka spill site, Hungary. Environ. Sci. Technol. 46, 3085–3092.

Damayanti, R., Khaerunissa, H., 2017. Composition and characteristics of red mud: a case study on Tayan bauxite residue from alumina processing plant at West Kalimantan. Indones. Min. J. 19, 179–190.

Dubovikov, O.A., Jaskelainen, E.E., 2016. Processing of low-quality bauxite feedstock by thermochemistry-Bayer method. J. Min. Inst. 221, 668–674.

Evans, A.M., 1993. Ore Geology and Industrial Minerals: An Introduction. Blackwell Science.

Gow, N.N., Lozej, G.P., 1993. Bauxite. Geosci. Can. 20, 9–16.

Heryanto, R., Margono, U., 2008. The provenance and diagenesis of sandstones of the Eocene Tanjung Formation in the Kualakurun area, Central Kalimantan. Geol. Surv. Inst. 18, 291–298.

Jaya, A.F., Rumapea, M.P., Akbar, N.K., 2020. Implementasi integrasi proses pengolahan bauksit dan pemanfaatan red mud di Tayan, Kalimantan Barat untuk Indonesia maju 2045. Pros. Temu Prof. Tah. PERHAPI 653.

Kementerian ESDM, 2024. Pemilik cadangan nikel dan bauksit terbesar di dunia, ini yang dilakukan Indonesia. Kementerian Energi dan Sumber Daya Mineral. https://www.esdm.go.id/id/media-center/arsip-berita/pemilik-cadangan-nikel-dan-bauksit-terbesar-di-dunia-ini-yang-dilakukan-indonesia (Accessed 15 August 2025).

Lintjewas, L., Setiawan, I., Kausar, A., 2019. Profil endapan nikel laterit di daerah Palangga, Provinsi Sulawesi Tenggara. Ris. Geol. Pertamb. 29, 91–104. https://doi.org/10.14203/risetgeotam2019.v29.970

Moskalyk, R.R., Alfantazi, A.M., 2003. Processing of vanadium: a review. Miner. Eng. 16, 793–805.

Nabilah, A., 2022. Pengayaan critical raw materials pada endapan bauksit dan residunya di daerah Tayan, Kabupaten Sanggau, Kalimantan Barat. Universitas Gadjah Mada.

Nurlela, K.A., Wijayanti, K., Hamdanillah, R.P., 2024. Hubungan batuan induk terhadap kadar alumina pada prospek X Kecamatan Nanga Tayap, Ketapang, Kalimantan Barat. Geosci. J. 8, 1797–1811.

Permatasari, A., Suprapto, S.J., Priatna, Handayani, T., Sunjaya, D., 2024. Geologi, mineralogi, dan geokimia endapan bauksit laterit di Desa Mukti Jaya, Kabupaten Sanggau, Kalimantan Barat. Bul. Sumber Daya Geol. 19, 121–130.

Praja, A.A., Tangahu, B.V., Yulikasari, A., Arliyani, I., Mashudi, Titah, H.S., Ramadhani, M.A., Fauziah, N.F., Lam, Y.M., Wang, Y., In, H., Soesilo, M.M., 2025. Phytomining potential of Jatropha curcas and Sansevieria trifasciata for chromium (Cr) and vanadium (V) uptake from red mud amended with sludge-manure mixture. BIO Web Conf. 157, 1–16.

Purnomo, H., Wijaya, R.A.E., 2022. Pemetaan sebaran kadar Al_2O_3 dan $RSiO_2$ pada endapan laterit bauksit menggunakan pendekatan metode interpolasi ordinary kriging dan inverse distance weighting. Angkasa J. Ilm. Bid. Teknol. 14, 75–86.

Ramadhan, F.R., Aribowo, Y., Widiarso, D.A., Sunjaya, D., 2014. Geologi, karakteristik dan genesa endapan bauksit PT. Antam, daerah Kenco, Kabupaten Landak, Provinsi Kalimantan Barat. J. Tek. Geol. Univ. Diponegoro 1–14.

Rizal, K., Idrus, A., 2024. Global critical mineral review and challenges on its exploration in Indonesia. Indones. Min. J. 27, 97–123.

Santi, M., 2019. Netralisasi air lindi residu bauksit (red mud) dengan menggunakan air gambut. J. Ilm. Teknosains 4, 76–79.

Setiawan, I., Estiaty, L., Fatimah, D., Indarto, S., Lintjewas, L., Alkausar, A., Handoko, A., Yuliyanti, A., Jakah, J., 2020. Geologi dan petrokimia endapan zeolit daerah Bayah dan Sukabumi. Ris. Geol. Pertamb. 30, 39–54. https://doi.org/10.14203/risetgeotam2020.v30.1048

Setiawan, N.I., Osanai, Y., Nakano, N., Adachi, T., Setiadji, L.D., Wahyudiono, J., 2013. Late Triassic metatonalite from the Schwaner Mountains in West Kalimantan and its contribution to sedimentary provenance in the Sundaland. Berita Sedimentol. 12, 4–12.

Solihin, S., Lisdiana, A., Dida, E., 2024. A systematic review of geological resource containing nickel: resource, distribution, mining, extraction and advanced material synthesis. Ris. Geol. Pertamb. 34, 97–110. https://doi.org/10.55981/risetgeotam.2024.1339

Sudana, D., Djamal, B., Sukido, 1994. Peta Geologi Lembar Kendawangan, Kalimantan Barat. Pusat Penelitian dan Pengembangan Geologi.

Suherman, I., Suseno, T., Saleh, R., 2015. Kajian manfaat usaha pertambangan bauksit terhadap sosial ekonomi daerah di Provinsi Kalimantan Barat. J. Teknol. Miner. Batubara 11, 129–145.

Syaputra, R., Santoso, A.B., 2024. Karakteristik geokimia endapan bauksit di daerah X, Kalimantan Barat, Indonesia. J. Teknol. Pertamb. Geosains 1, 29–35.

Valeton, I., 1972. Bauxites (Developments in Soil Science). Elsevier.

Van Bemmelen, R.W., 1949. The Geology of Indonesia. Martinus Nijhoff, The Hague.

Williams, P.R., Johnston, C.R., Almond, R.A., Simamora, W.H., 1988. Late Cretaceous to early Tertiary structural elements of West Kalimantan. Tectonophysics 148, 279–297.

Zaharah, T.A., Rossalina, W., Silalahi, I.H., 2021. Komposisi unsur dan karakterisasi mineral magnetik dalam red mud, residu bauksit di PT Indonesia Chemical Alumina (ICA) Kalimantan Barat. Indones. J. Pure Appl. Chem. 4, 139–144.